
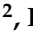




Article

# Immobilized Cell Physiology Imaging and Stabilization of Enzyme Cascade Reaction Using Recombinant Cells *Escherichia coli* Entrapped in Polyelectrolyte Complex Beads by Jet Break-Up Encapsulator

Marek Bučko <sup>1,\*</sup>, Peter Gemeiner <sup>1</sup>, Tomáš Krajčovič <sup>1</sup>, Marietta Hakarová <sup>1</sup>, Dušan Chorvát <sup>2</sup>, Alžbeta Marček Chorvátová <sup>2</sup>, Igor Lacík <sup>3</sup>, Florian Rudroff <sup>4</sup> and Marko D. Mihovilovič <sup>4</sup>

<sup>1</sup> Department of Glycobiotechnology, Institute of Chemistry, Slovak Academy of Sciences, Dúbravská cesta 9, 845 38 Bratislava, Slovakia; Peter.Gemeiner@savba.sk (P.G.); Tomas.Krajcovic@savba.sk (T.K.); mariett.hakarova@gmail.com (M.H.)

<sup>2</sup> Department of Biophotonics, International Laser Centre, Ilkovičova 3, 841 04 Bratislava, Slovakia; Dusan.Chorvat@ilc.sk (D.C.); Alzbeta.MarcekChorvatova@ilc.sk (A.M.C.)

<sup>3</sup> Polymer Institute, Slovak Academy of Sciences, Dúbravská cesta 9, 845 41 Bratislava, Slovakia; Igor.Lacik@savba.sk

<sup>4</sup> Institute of Applied Synthetic Chemistry, TU Wien, Getreidemarkt 9/163, 1060 Vienna, Austria; florian.rudroff@tuwien.ac.at (F.R.); marko.mihovilovic@tuwien.ac.at (M.D.M.)

\* Correspondence: Marek.Bucko@savba.sk; Tel.: +421-2-59410319

Received: 21 September 2020; Accepted: 2 November 2020; Published: 5 November 2020



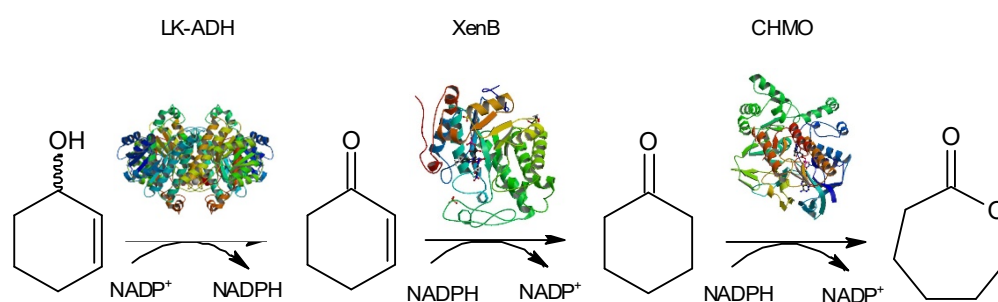
**Abstract:** A novel, high performance, and scalable immobilization protocol using a laminar jet break-up technique was developed for the production of polyelectrolyte complex beads with entrapped viable *Escherichia coli* cells expressing an enzyme cascade of alcohol dehydrogenase, enoate reductase, and cyclohexanone monooxygenase. A significant improvement of operational stability was achieved by cell immobilization, which was manifested as an almost two-fold higher summative product yield of 63% after five cascade reaction cycles as compared to the yield using free cells of 36% after the maximum achievable number of three cycles. Correspondingly, increased metabolic activity was observed by multimodal optical imaging in entrapped cells, which was in contrast to a complete suppression of cell metabolism in free cells after five reaction cycles. Additionally, a high density of cells entrapped in beads had a negligible effect on bead permeability for low molecular weight substrates and products of cascade reaction.

**Keywords:** enzyme cascade reaction; immobilization; polyelectrolyte; multimodal optical imaging; biocatalysis; whole-cell biocatalyst

## 1. Introduction

Research in the field of biocatalysts is progressing and currently has all the features of an advanced phase of the preparation for the so-called fourth wave of biocatalysis [1]. The assumption is that the “first choice” strategy in the field of biocatalysis will be a combination of enzymes either in cascade reactions or using metabolic engineering, including the use of immobilization techniques [1]. Whole-cell cascade biocatalysis has progressively been established as a viable alternative to metabolic engineering [2]. Several whole-cell enzyme cascade systems using the effect of shifting the reaction equilibrium using an irreversible reaction catalyzed by enzymes, in particular from the group of Baeyer–Villiger monooxygenases (BVMOs), have been reported to maximize the yield of the desired

product [3]; Scheme 1. Whole-cell BVMOs as catalysts for Baeyer–Villiger bio-oxidation have also enabled a stereoselective approach to the chemoenzymatic synthesis of bioactive compounds, including the non-natural C-nucleoside carba-showdomycin derived from the antibiotic showdomycin [4]. A form of glycosidic bonding in C-nucleosides such as showdomycin inspired the development of nucleoside analogs as potent antivirals, such as the BCX-4430 molecule against virus MERS [5]. It is apparent that the systematic development of antiviral nucleoside analogs in the past may be beneficial for the current rapid repurposing of drugs such as remdesivir and ribavirin for the COVID-19 pandemic [6]. Additionally, an important example of the use of BVMOs in the industry is the use of cyclohexanone monooxygenase for the production of the drug esomeprazole by Codexis for the treatment of severe gastrointestinal disorders [7].



**Scheme 1.** Model cascade reaction of 2-cyclohexenol catalyzed by recombinant viable cells *Escherichia coli* with the expressed alcohol dehydrogenase (LK-ADH), enoate reductase (XenB), and cyclohexanone monooxygenase (CHMO<sub>Acineto</sub>) enzymes entrapped in polyelectrolyte complex beads used in this work. Enzyme structures were adapted for illustrative purposes from the database [www.rcsb.org](http://www.rcsb.org).

The versatility of BVMOs, together with the utilization of protein engineering approaches, opens the way for applications of BVMOs in industry [8]. This development in the field of whole-cell biocatalysis is a good reason to continually develop and exploit the benefits of whole-cell immobilization, which has enabled the biocatalytic efficacy and economic efficiency of whole-cell biocatalysts to be improved by allowing for their continuous and/or repetitive use and the stabilization of cells [9]. Developments in the field of immobilization by entrapment and encapsulation techniques, rather than by continuously expanding the material base, have been focused on improving the properties of existing systems. Attention has been paid to increasing the resistance and regulation of matrix permeability by silicating [10], gelling alginate with other cations [11], combining polymers to facilitate immobilization [12], changing encapsulation conditions to cell entrapment [13], and designing hydrogel particles for other uses such as drug delivery [14]. Additionally, the scale-up of hydrogel particle productivity from laboratory quantities to the operational scale is an important part of the development of immobilized whole-cell biocatalysts. Current commercially available high-performance devices operate by different physical principles of bead production such as the production of droplets by coaxial air-stripping nozzle, the breaking of the hydrogel flow using superimposed electromagnetic vibrations, or jet-cutting by high speed cutting wire [15].

The use of the immobilization of viable recombinant cells with overproduced BVMO enzymes has contributed to cell stabilization and recyclability [3]. The introduction of the two-step production of polyelectrolyte (PEC) particles with immobilized *Escherichia coli* cells with BVMO, in addition to cell stabilization, has reduced the consumption of immobilization materials and simplified the immobilization procedure [16]. Considering the progress in the development of immobilized whole-cell biocatalysts [17,18] and the mentioned stabilizing effect using immobilization for BVMOs, there is a rational assumption that immobilization in polyelectrolyte complex beads may create benefits from the stabilization of recombinant whole-cells with expressed cascade enzymes selected for this work. The fine-tuned non-natural cascade system *E. coli* BL21 (DE3) (pET28\_CHMO\_XenB + pET22b\_LKADH) of alcohol dehydrogenase (LK-ADH) from *Lactobacillus kefir*-enoate reductase (XenB) from *Pseudomonas*

*putida*-cyclohexanone monooxygenase (CHMO) from *Acinetobacter calcoaceticus* [19], which had not previously been attempted to be used repeatedly, was chosen as model for immobilization and repeated cascade reactions. The selected enzyme cascade for immobilization (Scheme 1) represents a continuation of the development of immobilized BVMO-based biocatalysts from one-step synthesis [17] to cascade systems. Moreover, the cofactor-regenerating cascade system based on LK-ADH, which simultaneously regenerates nicotinamide adenine dinucleotide phosphate (NADPH) by cellular metabolism for the other two cascade reactions [19], appears to be suitable model for the application of multimodal optical imaging to characterize the physiological processes in cells during catalysis.

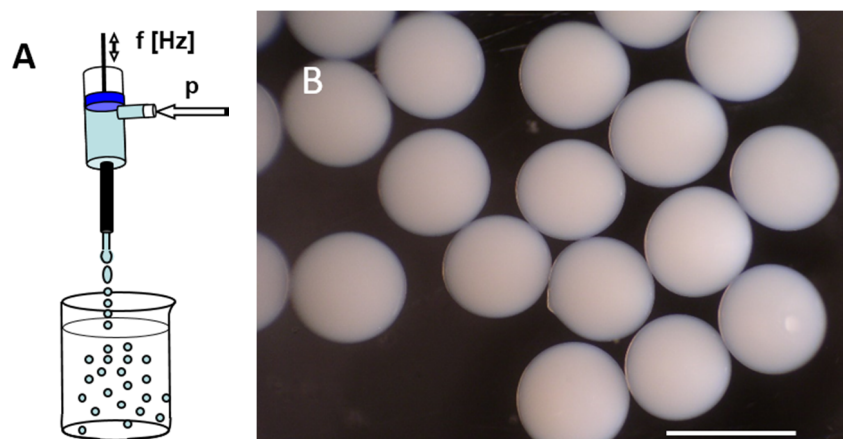
Regarding the development of characterization methods for immobilized whole cell biocatalysts used in biotransformation processes [20,21], there is a constant need for truly non-invasive microscopic techniques for the real-time imaging of living cells. In this regard, fluorescence microscopy allows for the imaging of cellular structures and polymer matrices with sub-micrometer resolution, while retaining high specificity and sensitivity in their native (liquid) environment. Several major developments have been introduced in the past few decades to improve the spatial resolution, specificity, and sensitivity of fluorescence microscopy. Laser scanning, confocal detection, non-linear excitation, super-resolution, or multi-modal approaches are the most pronounced examples. The application of ultrafast pulsed lasers, fast photon-counting detectors, and advanced electronics has resulted in the ability to differentiate fluorescence photons by several parameters simultaneously, leading to various modes of detection such as spectrally-resolved and fluorescence lifetime imaging [22]. These advances, together with new biophysical approaches of probe design allows one to achieve a deep insight into cellular physiology. One of the most promising fields of current development is the application of advanced optical techniques to decipher intrinsic (natural) cell fluorescence for metabolic studies [23].

The aim of this work was to immobilize recombinant viable cells *E. coli* with enzyme cascades within polyelectrolyte complex beads and to develop an innovative immobilization protocol for their production with a high throughput. The operational stability of entrapped cells during repeated cycles of a model cascade reaction was investigated. Additionally, new insight into immobilized cell physiology was performed by utilizing multimodal optical imaging. The influence of the cell presence on the molecular weight cut-off of PEC beads was determined.

## 2. Results

### 2.1. Production of PEC Beads with Entrapped *E. coli* Containing Enzyme Cascade ADH, XenB, and CHMO Using Jet Break-Up Technique

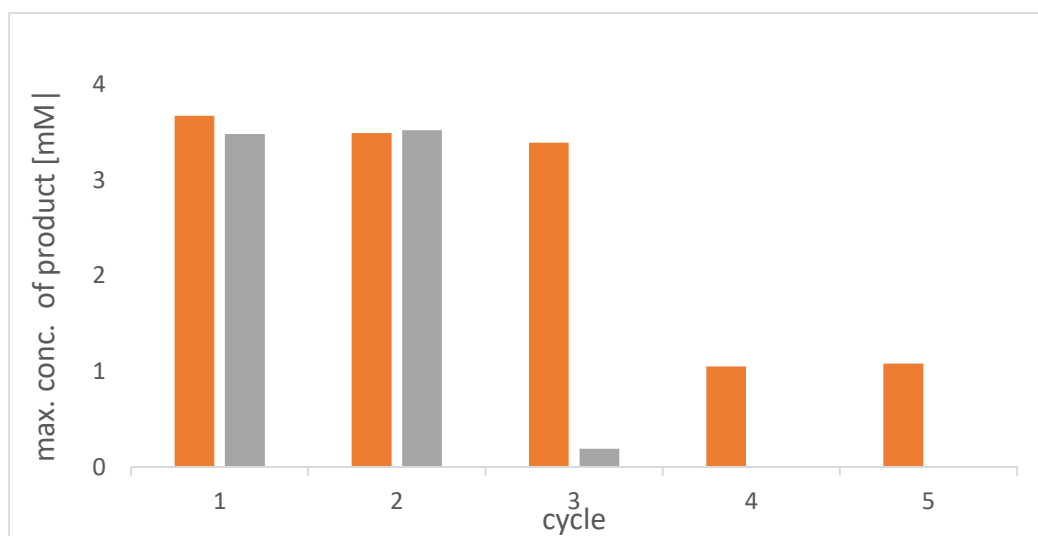
The production of polyelectrolyte complex (PEC) beads in easy scalable manner to prove the potential applicability of entrapped viable cells in biotechnological processes is challenging task. It requires the balanced consideration of many parameters such as the choice and characterization of immobilization polymers, their concentration, cell concentration, gelation and complexation time, and the use of scalable extrusion techniques with emphasis on potential cost savings. A novel, high performance immobilization protocol was developed for the production of PEC beads with entrapped viable *E. coli* cells expressing the recombinant enzymes using a high performance encapsulator based on the laminar jet break-up technique (Figure 1A). A two-step immobilization procedure was adapted using an encapsulator with a 15-fold higher throughput of 15 mL/min as compared to a previously used air-stripping nozzle [17]. This immobilization procedure is also easily scalable by the multiplication of nozzle number of the encapsulator. Moreover, cost and material savings were achieved with about a 10-fold decrease in consumption of poly(methylene-co-guanidine) PMCG and washing solutions as compared to a previous immobilization protocol [17]. As a result, uniform PEC beads with entrapped viable *E. coli* cells containing the LK-ADH, XenB, and CHMO enzyme cascade with a diameter of  $0.8 \pm 0.15$  mm were produced (Figure 1B).



**Figure 1.** (A) The laminar jet break-up technique ( $f$  = frequency of pulsation membrane;  $p$  = pressure of polyanion (PA) solution with cells), used for preparation of polyelectrolyte (PEC) beads with entrapped cells (10% wt.) *E. coli* with the LK-ADH, XenB, and CHMO enzyme cascade (B). Average bead diameter is  $0.8 \pm 0.15$  mm. Length of a white bar corresponds to 1 mm.

## 2.2. Operational Stability of PEC Beads with Entrapped *E. coli* Containing Enzyme Cascade

For the first time, the operational stability of entrapped recombinant cells with the LK-ADH, XenB, and CHMO enzyme cascade was tested and compared with the operational stability of free cells. Clear  $LB_{amp+kan}$  media from cell isolation were reused for the preparation of reaction mixtures instead of fresh buffered media, which may have improve the economy of the process. The immobilization of *E. coli* cells expressing the recombinant enzymes in PEC particles allowed for the reuse of the immobilized cells in up to five catalysis of the 2-cyclohexen-1-ol cascade reaction to  $\epsilon$ -caprolactone. The re-utilization performances of the free cells rapidly decreased, being almost completely inactive after the third round (Figure 2). The gradual decrease of biocatalytic efficacy in both free and entrapped cells was manifested by prolonging the reaction time that was necessary to reach the maximum concentration of the product from 6 h in the first reaction cycle to 48 h in the third cycle (free cells) and the fifth cycle (entrapped cells), respectively. Regardless of this, the sum of the  $\epsilon$ -caprolactone yields, based on gas chromatography, was almost two-fold after five repeated cascade reaction cycles that utilized entrapped cells (36.2 mg) as compared to free cells (20.5 mg). The sensitivity of the enzyme cascade to the repetition of transformations may explain the lower operational stability of this system compared to recombinant cells with the single BVMO enzyme used previously [16]. Nevertheless, it can be concluded that the stabilization effect of cell immobilization during cascade cycles is apparent.



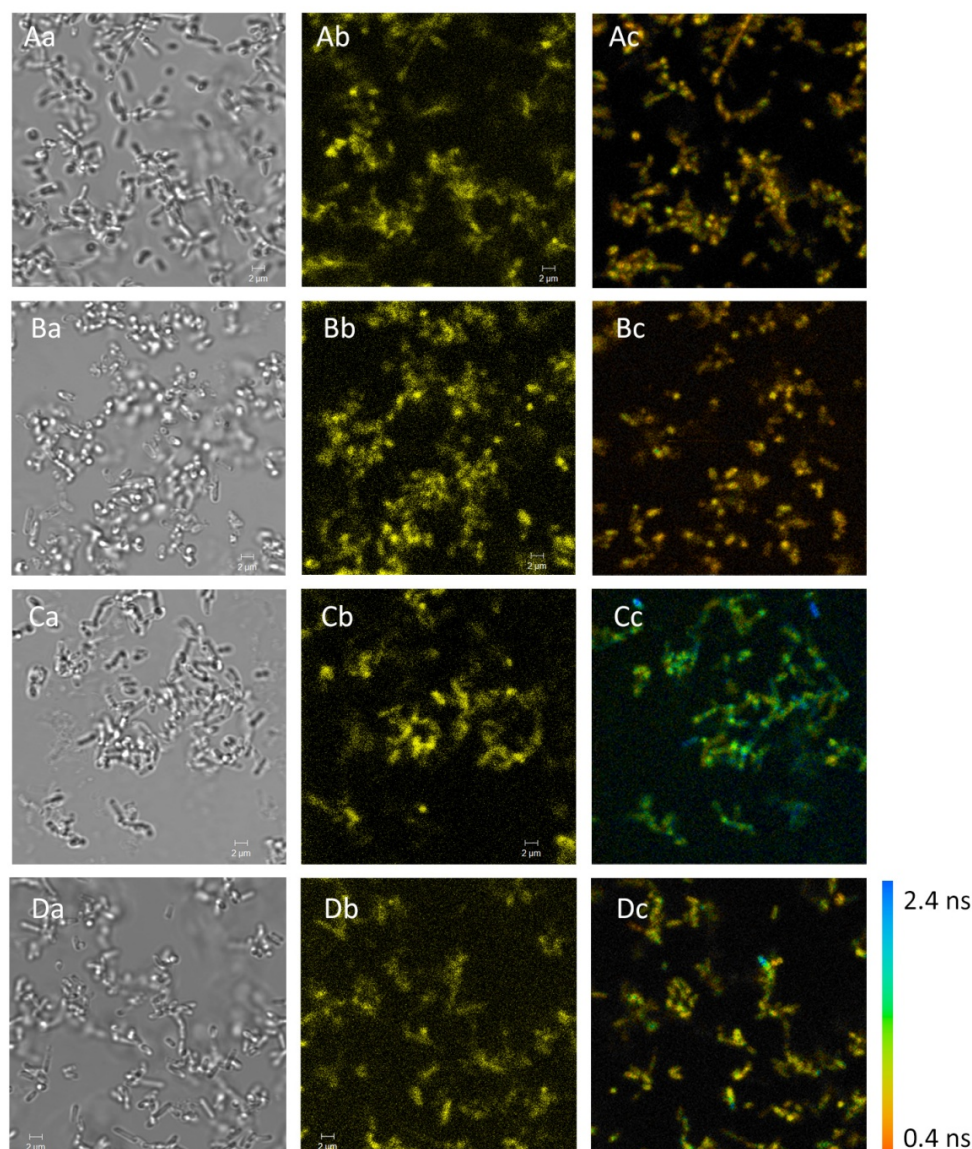
**Figure 2.** Operational stability of viable cells *E. coli* with LK-ADH, XenB, and CHMO enzyme cascade entrapped in PEC beads (orange columns) and free cells (gray columns) during repeated cycles of model cascade reaction of 2-cyklohexen-1-ol to  $\epsilon$ -caprolactone, depicted as the maximum achieved product concentration. Biotransformation conditions: temperature of 24 °C, orbital shaking at 200 rpm in LB<sub>amp+kan</sub> media supplemented with 1% glucose with a pH of 7 and an initial substrate concentration of 4 mM. One-hundred percent activity of free cells was retained in PEC beads immediately after cell immobilization; this equaled a specific activity  $A = 1.2$  U/mg (for free cells) and  $A = 0.24$  U/mg (for PEC beads with cells).

### 2.3. Metabolic Assessment of *E. coli* Using Multi-Modal Optical Imaging

In our previous work, confocal microscopy imaging was used to characterize the polymer capsules and viability of encapsulated cells [17]. In this study, we applied, for the first time, an advanced multi-modal optical imaging to assess the metabolic state of *E. coli* cells during the biotransformation process. To follow this aim, we evaluated the intrinsic fluorescence of flavins, for which the characteristic excitation and emission ranges are 440–480 and 500–550 nm, respectively.

The initial attempt to utilize multispectral imaging showed insignificant changes in the emission spectra of *E. coli* in various conditions. This could mostly be attributed to the fact that free and bound flavin forms had strongly overlapping emission peaks and that the low signal from individual cells hampered the successful spectral unmixing of signals for both free and bound flavin forms in our experimental setup. A different situation was met when the fluorescence lifetime imaging (FLIM) method was used for the detection of fluorescence signal (Figure 3). After five cycles of cascade reaction in the free cells, a shortening of the mean fluorescence lifetime was observed (Figure 3Bc), which was in contrast to the significant increase of the same parameter in a large fraction of the entrapped cells (Figure 3Cc). Based on previously described characteristics of flavins with the short lifetime component, which corresponded to the bound forms, and the long-living component related to the free molecular conformations, we formulated the working hypothesis that Figure 3 depicts the decrease in the free flavin concentration in the case of free cells after biotransformation compared to the increased concentration of free flavins in *E. coli* cells entrapped in PEC beads. To test this hypothesis, we applied 10 mM glucose to the solution of control cells (Figure 3Dc) and observed that the mean lifetime increased after the stimulation of the cell metabolism by glucose.

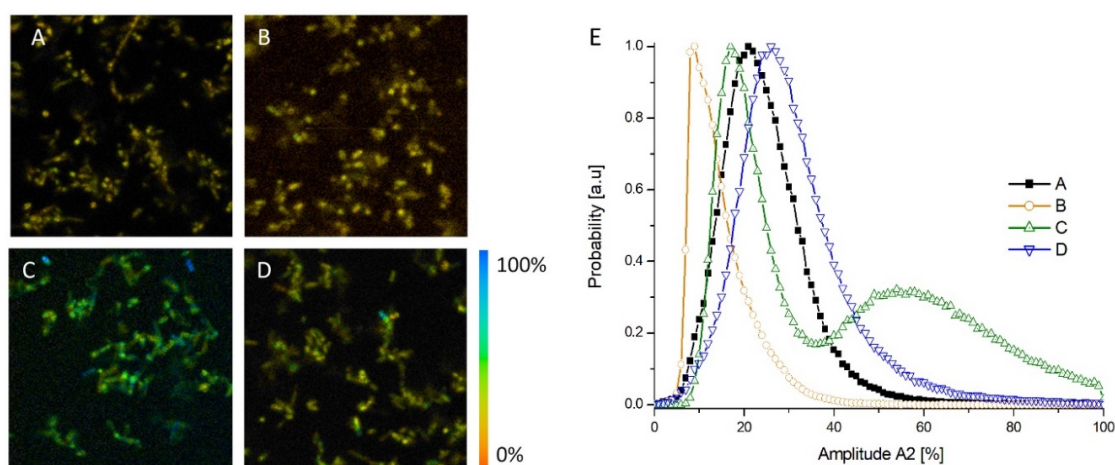




**Figure 3.** *E. coli* cells imaged by optical microscopy in control conditions (A), after 5 cycles of cascade reaction in free cells (B), after 5 cycles of cascade reaction in entrapped cells (C), and in control cells with addition of 10 mM glucose (D). Optical contrast: transmission (a), fluorescence intensity (b), and mean fluorescence lifetime (c) color-coded according to the given scale.

In order to achieve a more quantitative evaluation of the observed effects, we performed a FLIM fluorescence decay analysis using two fixed exponential components (0.4 and 2.4 ns), mimicking the bound and free flavin forms, respectively. The relative concentration of the long-lifetime component could then be directly attributed to the percentage of the free flavins in the *E. coli* cells (Figure 4). The plot of the cumulative histograms of the relative amplitudes of 2.4 ns decay component (Figure 4E) from several experiments confirmed our conclusion that after the biotransformation, we saw the increased metabolic activity in a large portion of entrapped cells, while the complete suppression of metabolism was seen in free cells. Being an enzymatic co-factor in the oxidative reactions, flavin and NAD(P)H metabolism pathways are inversely proportional. Thus, the increase of free flavins corresponds to the increased consumption of NAD(P)H and vice versa. We can therefore conclude that the consumption of NAD(P)H was completely suppressed in the free cells after biotransformation, while a significant portion of encapsulated cells retained their NAD(P)H catalytic activity even after

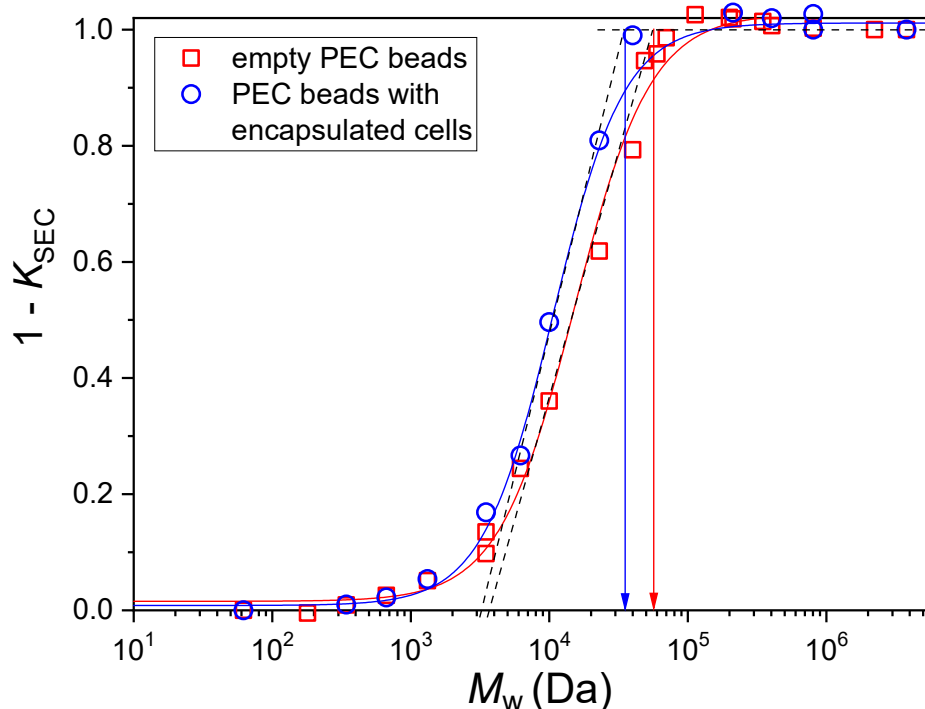
five cycles of cascade reaction. This conclusion corresponded well with the findings provided by other techniques used in this study.



**Figure 4.** Representative images of spatial distribution of the relative amplitudes of long-lifetime component estimated from fluorescence lifetime imaging (FLIM) images: control conditions (A), after 5 cycles of cascade reaction-free cells (B), after 5 cycles of cascade reaction in entrapped cells (C), and control cells with addition of 10 mM glucose (D). Cumulative histogram of the relative amplitudes of long-lifetime decay component (E) corresponding to cells in cases (A–D). Distributions were computed from  $N = 4\text{--}7$  images and normalized to their respective maximum.

#### 2.4. Influence of Cell Immobilization on MWCO of PEC Beads

The principle of the cell entrapment in PEC beads allows for the immobilization and preconcentration of a very high cell content that maximizes the biocatalytic efficiency with respect to the volume of a biocatalytic system. On the other hand, the immobilization principle has to consider the permeability characteristics, i.e., the requirement of the controlled and effective exchange of substrates, nutrients, and products between the bead volume and the bead environment. Since the composition and size of the developed PEC particles were optimized [16], the cell concentration was another variable in the design of the immobilization system in this work. The high concentration of wet *E. coli* cells with the LK-ADH, XenB, and CHMO cascade in the 10 wt.% PEC beads was the maximum possible concentration in view of the feasibility of creating a uniform droplet stream using a high performance encapsulator. The possible effect of the presence and concentration of cells on the permeability of PEC beads was examined using the inverse size-exclusion chromatography technique (iSEC) that provides information on the matrix molecular weight cut-off (MWCO) [24]. Figure 5 reveals a comparison between the cumulative pore size distributions curves for empty PEC beads and for beads containing 10 wt.% of immobilized cells *E. coli* with the enzyme cascade; this could be used for evaluation of MWCO values [25,26]. For the beads containing cells, the shift of the separation part of the curve to the lower molecular weight values compared to the empty beads evidenced that the cell-loaded beads were less permeable. This was expressed in the MWCO values that were ~35 and 60 kDa for the beads with immobilized cells and empty beads, respectively. These values were based on the permeation of pullulan standards and could be transformed into the molecular weight of proteins [24] that are ~150 and 300 kDa, respectively. These values indicate that the permeation of low molecular weight substrate and product through the immobilization matrix should not be restricted. The difference between the permeability characteristics of empty and loaded beads could have resulted from the hydrogel network re-arrangement [27] that is natural for this type of non-covalently stabilized networks and may have been influenced by the presence of cells.



**Figure 5.** Cumulative pore size distributions determined by an inverse size-exclusion chromatography for PEC empty beads and entrapped *E. coli* cells expressed by the experimental data ( $1 - K_{SEC}$ ), where  $K_{SEC}$  represents the chromatographic partition coefficient against the molecular weight of pullulan standards. The data were fitted with the Boltzmann function. The matrix molecular weight cut-off (MWCO) values for respective bead types are marked by arrows and were determined following the work of Brissova et al. [25].

### 3. Materials and Methods

#### 3.1. Immobilization Polymers, Media and Chemicals

High-viscosity, high-mannuronic acid sodium alginate from ISP Alginate (Girvan, UK), PMCG from Scientific Polymer Products Inc. (Ontario, NY, USA), supplied as a 35% (w/v) aqueous solution and lyophilized prior to use. Additionally, water-soluble cellulose sulfate (CS) with the required degree of substitution (DS), dynamic viscosity, and MW were provided by Senova Biotechnologieunternehmen (Weimar, Germany) and used for cell immobilization. All mentioned polymers were characterized as previously reported in detail [17]. The substrate, 2-cyclohexenol (Aldrich, St. Louis, MO, USA), and the analytical standards of cascade reaction products, 2-cyclohexenone (Aldrich, Darmstadt, Germany), cyclohexanone (Sigma-Aldrich, Darmstadt, Germany), and  $\epsilon$ -caprolactone (Aldrich, St. Louis, MO, USA), were purchased from Sigma-Aldrich (Bratislava, Slovakia). Cell media [19]: the  $LB_{amp+kan}$  agar Petri dish contained 10 g/L of peptone (Oxoid, Hampshire, UK), 5 g/L of yeast extract (Oxoid, Hants, UK), 10 g/L of NaCl (Slavus, Bratislava, Slovakia), 15 g/L of agar (Oxoid, Hampshire, UK), 100  $\mu$ g/mL of ampicillin (Sigma-Aldrich, Madrid, Spain), and 50  $\mu$ g/mL of kanamycin (Sigma, Jerusalem, Israel). The  $LB_{amp+kan}$  medium for cell growth had the same composition, without agar. The  $TB_{amp+kan}$  for cell production medium contained 12 g/L of tryptone (Oxoid, Hampshire, UK), 24 g/L of yeast extract, 5 g/L of glycerol (Sigma, Subang Jaya, Malaysia), 16.4 g/L of  $K_2HPO_4 \cdot 3H_2O$  (Carl Roth, Karlsruhe, Germany), 2.3 g/L of  $KH_2PO_4$  (Slavus, Bratislava, Slovakia), 100  $\mu$ g/mL ampicillin, and 50  $\mu$ g/mL kanamycin. Isopropyl  $\beta$ -D-1-thiogalactopyranoside (IPTG) (0.1 mM) was from Takara Bio Inc. (Otsu, Japan). All other chemicals and solvents were provided by commercial suppliers.



### 3.2. Cultivation of Cells

The recombinant *E. coli* BL21 (DE3) (pET28\_CHMO\_XenB and pET22b\_LKADH) strain overexpressing the enzyme cascade of LK-ADH from *Lactobacillus kefir*, XenB from *Pseudomonas putida*, and CHMO from *Acinetobacter calcoaceticus* was kindly donated by Professor Marko D. Mihovilovič (TU Vienna, Vienna, Austria). Cells were cultivated as reported previously [19]. Briefly, cells were streaked on an LB<sub>amp+kan</sub> agar Petri dish and incubated at 37 °C for 12 h. A single colony was inoculated to a 10 mL of the LB<sub>amp+kan</sub> medium in an Erlenmeyer flask and allowed to grow at 37 °C in an orbital shaker at 200 rpm for 12 h. One percent of the inoculum (v/v) was pipetted into a TB<sub>amp+kan</sub> medium and cultivated at 37 °C in an orbital shaker at 200 rpm until the cell density reached an OD<sub>600</sub> of 0.7. Subsequently, 0.1 mM IPTG was added to the medium, and the culture was incubated at 25 °C in an orbital shaker at 200 rpm for 20 h. The cells were harvested by centrifugation from the medium at 15 °C and 4000 rpm for 15 min and used for cascade reactions and immobilization.

### 3.3. Preparation of Polyelectrolyte Complex Beads

A suspension of cells was added to a solution of polyanion (PA) consisting of 0.9% (w/v) of sodium alginate and 0.9% of CS in 0.9% (w/v) NaCl at pH = 7 to the final concentration of 10% of wet cells. A laminar jet of the PA solution with the cells was broken into the monodisperse drops by the superimposed vibrations using high performance Encapsulator Startup (EncapBioSystems Inc., Greifensee, Switzerland) into a stirred gelation solution of 1.0% (w/v) of CaCl<sub>2</sub>. The flow rate of PA solution with cells was 15 mL/min, and the vibration frequency was 550 Hz. The time of gelation was 10 min, and the collection time was 1 min. Subsequently, the prepared beads were separated from the gelation solution and transferred into a stirred solution containing 1.8% (w/v) of PMCG and 0.9% (w/v) of NaCl at pH = 7 for 10 min. The obtained polyelectrolyte complex beads were washed with 0.9% (w/v) of NaCl and stored in 0.9% (w/v) of NaCl at 4 °C. The preparation and storage of empty PEC beads was performed with the same procedure except for the addition of cells. The amount of immobilized cells in beads was 10% w/w (wet cells), which corresponded to 1% w/w of dry cells.

### 3.4. Repeated Biotransformations

Two grams of PEC beads with entrapped cells (10% w/w) and, parallelly, an equivalent amount of free *E. coli* cells were transferred into the TB<sub>amp+kan</sub> medium (pH = 7) with the volume of reaction mixture of 20 mL for both free and immobilized cells. The mixture was supplemented by 1% glucose and 4 mM of substrate in a closed flask with a 10-fold higher volume than that of the reaction mixture [19]. The model cascade reaction was initiated by the addition of the 2-cyclohexenol substrate in ethanol (volume ratio 1:9) to the reaction medium. The reaction conditions were 24 °C and 200 rpm in an orbital shaker. The reaction mixture was extracted in ethyl acetate, with methyl benzoate as the internal standard (0.5 mg/mL) and analyzed using gas chromatography (GC) [19] utilizing Agilent technologies 7890A GC system (Agilent technologies, Santa Clara, CA, USA). After each cycle of the cascade reaction, the PEC beads containing cells and the free cells were separated from the reaction medium by filtration (encapsulated cells) or centrifugation (free cells), washed with a substrate-free medium, and used for the next reaction cycle.

One unit of enzyme activity corresponded to production of 1 μmol of ε-caprolactone per hour under the experimental conditions.

### 3.5. Multi-Modal Optical Imaging

All experiments were performed on glass coverslips after *E. coli* immobilization to the glass surface using 0.2% polyethyleneimine from Sigma-Aldrich (Bratislava, Slovakia). Cells were kept in a neutral physiological solution in all cases except for the addition of 10 mM glucose in specified experiments. Confocal laser scanning microscopy (CLSM) images of bacteria were acquired using an Axiovert 200 M microscope and an LSM 510 Meta scanning head (Zeiss, Jena, Germany) equipped

with a C-Apochromat W corr. 40 × lens with numerical aperture of 1.2. Individual cells were excited with a 445 nm laser 445LM-100 (Kvant, Bratislava, Slovakia) and recorded either by photodiode (light transmission) or photomultiplier (fluorescence) with a long-pass LP-505 nm filter (Zeiss, Jena, Germany). For multispectral detection, we used a 16-channel META detector in the range of 490–650 nm.

Fluorescence lifetime imaging microscopy images were recorded using the time-correlated single photon counting (TCSPC) technique following excitation with a 473 nm picosecond laser diode (BDL-473, Becker & Hickl, Germany) with a 50 MHz repetition rate and an approximately 60 ps pulse length. The laser beam was directed to the excitation fiber of the LSM 510 confocal microscope, and the emitted fluorescence was collected with an external fiber port, filtered by the LP-500 nm filter, and detected by an HPM 100-40 photomultiplier with an SPC-830 TCSPC board (both Becker & Hickl, Berlin, Germany). For CLSM imaging, we used an image resolution of 512 × 512 pixels over a 45 × 45 μm sample area. For FLIM imaging, we used the same physical image area and a 256 × 256 pixel resolution.

### 3.6. Inverse Size Exclusion Chromatography (iSEC)

The molecular weight cut-off (MWCO) determination of PEC beads with and without immobilized cells was performed using the iSEC, technique as reported previously [26].

## 4. Conclusions

This work was aimed at the development of an immobilization process for recombinant *E. coli* cells harboring the multi-enzymatic cascade system, as well as the measurement of their operational stability during cascade reaction cycles. An easily scalable procedure and material saving was achieved using a laminar jet break-up encapsulator. It is also important that the achieved high cell density within the PEC beads had a negligible effect on the free substrate and product permeation through the beads. The operational stability of the free and immobilized cells with enzyme cascade of alcohol dehydrogenase, enoate reductase, and cyclohexanone monooxygenase was assessed. Significant improvements of operational stability and product yield were achieved by the immobilization of cells in PEC beads. The full mechanism of slowing the deactivation of the enzyme cascade, which was manifested by the suppression of NAD(P)H consumption in free cells and the retainment of NAD(P)H activity in immobilized cells, remains to be solved. Additionally, PEC particles could possibly serve as a barrier to contact with the dispersed phase in multiphase reactors, which are promising for increasing the productivity of bioprocesses [28]. An advanced multi-modal optical imaging process to assess the metabolic state of *E. coli* cells during the biotransformation process was also used for the first time. This method revealed that in the free cells, after several repeated biotransformation cycles, suppressed cell metabolism was observed; meanwhile, in entrapped cells after the same biotransformation process, the metabolic activity was retained in a significant portion of the cell population. It is therefore apparent that the introduction of multi-modal optical imaging, performed in this work, may become a new and powerful tool in the investigation and optimization of metabolic effects achieved by the immobilization of viable cells.

**Author Contributions:** Conceptualization, methodology, and writing—original draft preparation, M.B. and P.G.; T.K. and M.H. performed experiments and analyzed data; D.C. and A.M.C. designed experiments and wrote the manuscript; I.L. designed experiments and reviewed and edited the manuscript; F.R. and M.D.M. contributed know-how and materials, and they reviewed and edited the manuscript. All authors have read and agreed to the published version of the manuscript.

**Funding:** This work was supported by the Slovak Grant Agency for Science VEGA 2/0130/20 and by the Slovak Research and Development Agency under contract no. APVV-15-0227. The authors thank to Dušana Treľová, PhD. for measurements of MWCO of PEC beads.

**Conflicts of Interest:** The authors declare no conflict of interest.

## References

1. Bornscheuer, U.T. The fourth wave of biocatalysis is approaching. *Philos. Trans. R. Soc. A Math. Phys. Eng. Sci.* **2017**, *376*, 20170063. [[CrossRef](#)] [[PubMed](#)]
2. Rudroff, F. Whole-cell based synthetic enzyme cascades—light and shadow of a promising technology. *Curr. Opin. Chem. Biol.* **2019**, *49*, 84–90. [[CrossRef](#)] [[PubMed](#)]
3. Bučko, M.; Gemeiner, P.; Schenk Mayerová, A.; Krajčovič, T.; Rudroff, F.; Mihovilović, M.D. Baeyer-Villiger oxidations: Biotechnological approach. *Appl. Microbiol. Biotechnol.* **2016**, *100*, 6585–6599. [[CrossRef](#)] [[PubMed](#)]
4. Bianchi, D.A.; Morán-Ramallal, R.; Iqbal, N.; Rudroff, F.; Mihovilovic, M.D. Enantiocomplementary access to carba-analogs of C-nucleoside derivatives by recombinant baeyer–villiger monooxygenases. *Bioorg. Med. Chem. Lett.* **2013**, *23*, 2718–2720. [[CrossRef](#)] [[PubMed](#)]
5. Seley-Radtke, K.L.; Yates, M.K. The evolution of nucleoside analogue antivirals: A review for chemists and non-chemists. Part 1: Early structural modifications to the nucleoside scaffold. *Antivir. Res.* **2018**, *154*, 66–86. [[CrossRef](#)] [[PubMed](#)]
6. Guy, R.K.; DiPaola, R.S.; Romanelli, F.; Dutch, R.E. Rapid repurposing of drugs for COVID-19. *Science* **2020**, *368*, 829–830. [[CrossRef](#)]
7. Bong, Y.K.; Clay, M.D.; Collier, S.J.; Mijts, B.; Vogel, M.; Zhang, X.; Hang, X.; Zhu, J.; Nazor, J.; Smith, D. Synthesis of Pyrazole Compounds. U.S. Patent WO2011/071982 A2, 16 June 2011.
8. Schmidt, S.; Bornscheuer, U.T. Baeyer-Villiger monooxygenases: From protein engineering to biocatalytic applications. In *Peptidomics of Cancer-Derived Enzyme Products*; Elsevier BV: Amsterdam, The Netherlands, 2020; pp. 187–6047.
9. Kisukuri, C.M.; Andrade, L.H. Production of chiral compounds using immobilized cells as a source of biocatalysts. *Org. Biomol. Chem.* **2015**, *13*, 10086–10107. [[CrossRef](#)]
10. Guzzon, R.; Carturan, G.; Krieger-Weber, S.; Cavazza, A. Use of organo-silica immobilized bacteria produced in a pilot scale plant to induce malolactic fermentation in wines that contain lysozyme. *Ann. Microbiol.* **2011**, *62*, 381–390. [[CrossRef](#)]
11. Mørch, Y.A.; Donati, I.; Strand, B.L.; Skjåk-Braek, G. Effect of  $\text{Ca}^{2+}$ ,  $\text{Ba}^{2+}$ , and  $\text{Sr}^{2+}$  on Alginate Microbeads. *Biomacromolecules* **2006**, *7*, 1471–1480. [[CrossRef](#)]
12. Liu, H.; Duan, W.-D.; De Souza, F.Z.R.; Liu, L.; Chen, B.-S. Asymmetric Ketone Reduction by Immobilized *Rhodotorula mucilaginosa*. *Catalysts* **2018**, *8*, 165. [[CrossRef](#)]
13. Buchholz, K.; Kasche, V.; Bornscheuer, U.T. *Immobilization of microorganisms and cells: In Biocatalysts and Enzyme Technology*; Wiley-VCH: Weinheim, Germany, 2005; pp. 283–284, ISBN 3-527-30497-5.
14. Auriemma, G.; Russo, P.; Del Gaudio, P.; García-González, C.; Landín, M.; Aquino, R.P. Technologies and formulation design of polysaccharide-based hydrogels for drug delivery. *Molecules* **2020**, *25*, 3156. [[CrossRef](#)] [[PubMed](#)]
15. Prüsse, U.; Bilancetti, L.; Bučko, M.; Bugarski, B.; Bukowski, J.; Gemeiner, P.; Lewińska, D.; Manojlovic, V.; Massart, B.; Nastruzzi, C. Comparison of different technologies for alginate beads production. *Chem. Pap.* **2008**, *62*, 364–374. [[CrossRef](#)]
16. Krajčovič, T.; Bučko, M.; Vikartovska, A.; Lacik, I.; Uhelská, L.; Chorvát, D.; Neděla, V.; Tihlaříková, E.; Gericke, M.; Heinze, T.J. Polyelectrolyte Complex Beads by Novel Two-Step Process for Improved Performance of Viable Whole-Cell Baeyer-Villiger Monooxygenase by Immobilization. *Catalysts* **2017**, *7*, 353. [[CrossRef](#)]
17. Polakovič, M.; Švitel, J.; Bučko, M.; Filip, J.; Neděla, V.; Ansorge-Schumacher, M.B.; Gemeiner, P. Progress in biocatalysis with immobilized viable whole cells: Systems development, reaction engineering and applications. *Biotechnol. Lett.* **2017**, *39*, 667–683. [[CrossRef](#)]
18. Silva, A.L.P.; Caridade, T.N.D.S.; Magalhães, R.R.; De Sousa, K.T.; De Sousa, C.C.; Vale, J.A. Biocatalytic production of  $\epsilon$ -caprolactone using *Geotrichum candidum* cells immobilized on functionalized silica. *Appl. Microbiol. Biotechnol.* **2020**, 1–9. [[CrossRef](#)]
19. Oberleitner, N.; Peters, C.; Muschiol, J.; Kadow, M.; Saß, S.; Bayer, T.; Schaaf, P.; Iqbal, N.; Rudroff, F.; Mihovilovic, M.D. An enzymatic toolbox for cascade reactions: A showcase for an in vivo redox sequence in asymmetric synthesis. *ChemCatChem* **2013**, *5*, 3524–3528. [[CrossRef](#)]

20. Bučko, M.; Vikartovská, A.; Schenk Mayerová, A.; Tkáč, J.; Filip, J.; Chorvát, D.; Neděla, V.; Ansorge-Schumacher, M.B.; Gemeiner, P. Progress in emerging techniques for characterization of immobilized viable whole-cell biocatalysts. *Chem. Pap.* **2017**, *71*, 2309–2324. [[CrossRef](#)]
21. Neděla, V.; Tihlaříková, E.; Maxa, J.; Imrichová, K.; Bučko, M.; Gemeiner, P. Simulation-based optimisation of thermodynamic conditions in the ESEM for dynamical in-situ study of spherical polyelectrolyte complex particles in their native state. *Ultramicroscopy* **2020**, *211*, 112954. [[CrossRef](#)]
22. Becker, W. Errata to: Advanced Time-Correlated Single Photon Counting Applications. *Vibronic Interact. Mol. Cryst.* **2015**, *111*. [[CrossRef](#)]
23. Chorvat, D.; Chorvatova, A. Multi-wavelength fluorescence lifetime spectroscopy: A new approach to the study of endogenous fluorescence in living cells and tissues. *Laser Phys. Lett.* **2009**, *6*, 175–193. [[CrossRef](#)]
24. Brissova, M.; Petro, M.; Lacik, I.; Powers, A.C.; Wang, T. Evaluation of Microcapsule Permeability via Inverse Size Exclusion Chromatography. *Anal. Biochem.* **1996**, *242*, 104–111. [[CrossRef](#)]
25. Briššová, M.; Lacik, I.; Powers, A.C.; Anilkumar, A.V.; Wang, T. Control and measurement of permeability for design of microcapsule cell delivery system. *J. Biomed. Mater. Res.* **1998**, *39*, 61–70. [[CrossRef](#)]
26. Schenk Mayerová, A.; Bucko, M.; Gemeiner, P.; Trešová, D.; Lacik, I.; Chorvát, D.; Ačai, P.; Polakovič, M.; Lipták, L.; Rebroš, M. Physical and bioengineering properties of polyvinyl alcohol lens-shaped particles versus spherical polyelectrolyte complex microcapsules as immobilisation matrices for a whole-cell baeyer–villiger monooxygenase. *Appl. Biochem. Biotechnol.* **2014**, *174*, 1834–1849. [[CrossRef](#)]
27. Kroneková, Z.; Pelach, M.; Mazancová, P.; Uhelská, L.; Trešová, D.; Rázga, F.; Némethová, V.; Szalai, S.; Chorvát, D.; McGarrigle, J.J. Structural changes in alginate-based microspheres exposed to in vivo environment as revealed by confocal raman microscopy. *Sci. Rep.* **2018**, *8*, 1637. [[CrossRef](#)]
28. Melgarejo-Torres, R.; Pérez-Vega, S.; Rivera-Arredondo, V.M.; Che-Galicia, G. Multiphase bioreactors in the pharmaceutical industry. In *Modeling and Simulation of Heterogeneous Catalytic Processes*; Elsevier BV: Amsterdam, The Netherlands, 2019; Volume 54, pp. 195–237.

**Publisher's Note:** MDPI stays neutral with regard to jurisdictional claims in published maps and institutional affiliations.



© 2020 by the authors. Licensee MDPI, Basel, Switzerland. This article is an open access article distributed under the terms and conditions of the Creative Commons Attribution (CC BY) license (<http://creativecommons.org/licenses/by/4.0/>).